

A.A. PASICHNYI,¹ O.A. PRYGODIUK²

¹Institute for Nuclear Research, Nat. Acad. of Sci. of Ukraine
(47, Prosp. Nauky, Kyiv 03680, Ukraine; e-mail: apasichny@kinr.kiev.ua)

²Taras Shevchenko National University of Kyiv
(2, Academician Glushkov Prosp., Kyiv 03022, Ukraine)

**COULOMB RESONANCES,
QUASIREAL PHOTONS, AND GIANT
DIPOLE RESONANCE PHENOMENON**

PACS 25.30.Fj; 25.30.Dh

Various aspects of the influence of Coulomb resonances and quasireal photons on the dynamics of nuclear electro-disintegration by high-energy electrons have been studied in the framework of the nuclear shell model. Some peculiarities of numerical methods used to study the inelastic scattering cross-sections of high-energy electrons are also considered.

Keywords: Coulomb resonance, quasireal photons, giant dipole resonance phenomenon.

**1. Introduction:
Inelastic Scattering of High-Energy
Electrons by Atomic Nuclei**

Nowadays, the study of the processes of elastic and inelastic scattering of high-energy electrons by nuclei is known to be a source of the most reliable information on the structure of atomic nuclei [1–31]. The validity of this statement is supported by various theoretical and experimental factors. In the theoretical aspect, the weakness of the electromagnetic interaction between high-energy electrons and the nucleons of an atomic nucleus allows the reliability of the scattering theory formulas, which were obtained, as is known, in the framework of perturbation theory, to be considerably enhanced. At the same time, from the experimental viewpoint, physicists possess such experimental installations as highly effective beam accelerators of high-energy monoenergetic electrons. They also apply effective and recently improved methods to register charged particles in experiments dealing with the inelastic scattering of electrons by atomic nuclei accompanied, e.g., by the knockout of nucleons from nuclei (the reactions

$[A(e, e'p)A - 1]$ and $[A(e, e'n)A - 1]$). The perfection of the technique used to form highly intense beams of monoenergetic electrons in a wide range of energies, as well as to register those particles in nuclear experiments, plays a crucial role, when selecting projectile particles for an external action on the atomic nucleus in studies of the nuclear structure and properties: surely, these are high-energy electron beams. Hence, the application of the phenomenon of inelastic high-energy electron scattering by nuclei in order to study the structure of atomic nuclei may probably be, at the moment, the most effective method to obtain the comprehensive information on the atomic nucleus structure¹.

One of the research directions presented in this work is the elucidation of the basis to interpret the giant dipole resonance in the framework of the shell model of atomic nuclei, which was used earlier in a number of works [9, 18, 19, 29–31]. We will also try to be convinced that, in order to study the electronuclear phenomenon indicated above, it is possible to ef-

¹ Note that the highly intensive sources of monoenergetic beams of other particles that weakly interact with nucleons of atomic nuclei (neutrinos, photons, positrons) have not been yet created for today.

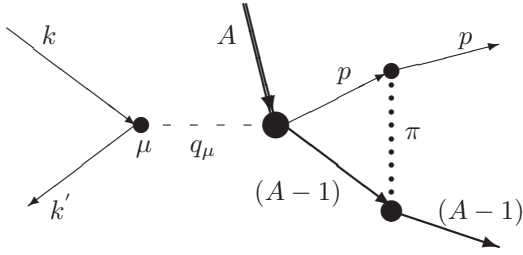


Fig. 1

ficiently use the phenomenon of inelastic high-energy electron scattering by atomic nuclei, provided that the experimental basis for studying the inelastic scattering of electrons with mass m and the initial and final energies ε and ε' at small angles θ' (the “0–0”-scattering [29, 31]),

$$\theta' \lll \frac{m(\varepsilon - \varepsilon')}{\varepsilon\varepsilon'} \lll 1, \quad (1)$$

would be extended.

The well-known phenomenon of giant dipole resonance [32] consists in the intense absorption of photons with a definite energy E_{dgr} ($7 \text{ MeV} \lesssim E_{\text{dgr}} \lesssim 23 \text{ MeV}$) by the nuclei of almost all chemical elements. Such absorption is reliably registered experimentally in rather a wide ($\sim 3 \div 5 \text{ MeV}$) energy interval (the giant resonance). Note that the most amazing property of the giant dipole resonance is the mentioned universality of this electronuclear phenomenon, namely, the absorption of photons by practically all ($A > 8$) atomic nuclei. It is also worth noting that the maximum energy of photon absorption, E_{dgr} , slightly exceeds 20 MeV ($E_{\text{dgr}} \lesssim 23 \text{ MeV}$) in the case of light atomic nuclei and gradually decreases to about 7 MeV ($E_{\text{dgr}} \gtrsim 7 \text{ MeV}$) for heavier atomic nuclei.

The conventional, at the moment, interpretation of the giant resonance phenomenon is constructed in the framework of the Migdal–Goldhaber–Teller model [32]. According to the hypothesis put forward by the indicated physicists, the phenomenon of photon absorption by atomic nuclei is accompanied by the excitations of collective motions in them, when the center of mass of all protons in the atomic nucleus shifts with respect to the center of mass of all neutrons in the same nucleus. We may assert that, despite its exotic nature, the Migdal–Goldhaber–Teller model [32] allows a significant progress in the interpreta-

tion of the giant dipole resonance phenomenon to be achieved².

In the present work with the help of the Coulomb resonance and quasireal photon concepts, we will try to interpret some specific features of the giant dipole resonance phenomenon by doing it in the framework of the shell model of atomic nucleus. We will also intend to propose a new method to study this phenomenon, while researching the inelastic scattering of high-energy electrons by nuclei. With that end in view, we recall below some properties of such concepts as Coulomb resonances and quasireal photons [9, 18, 19, 23, 29–31], which are rarely used. First of all, we note that, in the case of inelastic high-energy electron scattering, the electro-disintegration processes of atomic nuclei are described in a first approximation by the quantum-electrodynamic Feynman diagram depicted in Fig. 1. In what follows, we consider that the process of inelastic high-energy electron scattering by an atomic nucleus is accompanied by the transfer of the energy $\omega = \varepsilon - \varepsilon' > 0$, where ε and ε' are the electron energies before and after the inelastic scattering event, respectively, and the momentum $\mathbf{q} = \mathbf{k} - \mathbf{k}'$, where \mathbf{k} and \mathbf{k}' are the momenta of the scattered electron before and after its collision with the nucleus, respectively, to the target nucleus. We also consider that the magnitudes of transferred energy, ω , and momentum, $|\mathbf{q}|$, as well as the magnitude of the momentum of a knocked out nucleon, $|\mathbf{K}|$, satisfy the conditions: $\frac{\omega}{M} \lll 1$, $\frac{q}{M} \lll 1$, and $\frac{K}{M} \lll 1$.

Under the indicated assumptions, according to the diagram shown in Fig. 1, the process of inelastic electron scattering by the atomic nucleus A can be interpreted, e.g., as follows [30, 31]. An electron with the four-momentum $k \equiv k_\mu = (\mathbf{k}, i\varepsilon)$ approaches the atomic nucleus A , emits a virtual photon characterized by the four-momentum $q \equiv q_\mu = (\mathbf{q}, i\omega)$, and acquires the status of scattered electron with the four-momentum $k' \equiv k'_\mu = (\mathbf{k}', i\varepsilon') \equiv ((\mathbf{k} - \mathbf{q}), i(\varepsilon - \omega))$. Note that if the standard definition of a relativistic virtual photon mass is applied, $\omega^2 = \mathbf{q}^2 + m_f^2$,

² Note also that no interpretation of at least the main features of the giant dipole resonance phenomenon in the framework of the shell model of atomic nucleus has been given till now. One can hardly deny the fact that the “triumph” of the Migdal–Goldhaber–Teller model [32] in the interpretation of the giant dipole resonance phenomenon is associated with its unshakable monopoly in the indicated domain of theoretical nuclear physics.

we may assert that the mass m_f of a virtual photon is always determined by an imaginary number, since the inequality $\omega^2 < \mathbf{q}^2$ holds true for an arbitrary scattering angle [29]. Note that the mass m_f at fixed ε and ε' grows by absolute value with the angle of inelastic electron scattering θ' . In other words, the mass of a virtual photon moving along the direction of motion of the inelastically scattered electron is minimum.

The virtual photon mentioned above ($q \equiv q_\mu \equiv (\mathbf{q}, i\omega)$) is captured by one of the protons in the atomic nucleus. Occasionally, this proton can obtain the energy sufficient to overcome attractive nuclear forces and escape from the residual atomic nucleus ($A - 1$). The knocked out proton moves in the force field created by the atomic nucleus ($A - 1$), i.e. it is scattered by this nucleus by means of exchanging a hypothetical π -meson, as it is schematically shown in Feynman's diagram (Fig. 1).

In the framework of the nuclear shell model (the LS -coupling) under the conditions formulated above, the following formula can be obtained for the cross-section of high-energy electron scattering by nuclei [6, 18, 29–31] with the use of the McVoy–Van Hove interaction Hamiltonian [1, 2]:

$$\begin{aligned} \sigma_{xnl}(\mathbf{k}, \mathbf{k}', \mathbf{K}) &\equiv \frac{d^5 \sigma_{xnl}}{d\varepsilon' d\Omega' d\Omega} = \\ &= e^4 N_{xnl} F_x^2(q_\mu^2) \frac{4MK}{\mathbf{k}^2} \left[S_x(\mathbf{k}, \mathbf{k}', \mathbf{K}) \times \right. \\ &\left. \times P(\mathbf{k}, \mathbf{k}') G_{xnl}(\mathbf{q}, \mathbf{K}) \right], \end{aligned} \quad (2)$$

where e is the electron charge, N_{xnl} is the number of x -nucleons in the nuclear xnl -shell, $d\Omega' \equiv d\Omega_{\mathbf{k}'}$, $d\Omega \equiv d\Omega_{\mathbf{K}}$,

$$\theta' \equiv \theta_{\mathbf{k}'}, \quad \theta \equiv \theta_{\mathbf{K}}, \quad \theta_{\mathbf{k}} = 0, \quad (3)$$

$$\varphi' \equiv \varphi_{\mathbf{k}'} = 0, \quad \varphi_{\mathbf{q}} = \pi,$$

$$\gamma_x = 1.79\delta_{xp} - 1.91\delta_{xn}, \quad (4)$$

$$F_x(q_\mu^2) \equiv F(q_\mu^2) = (1 + 0.055(Fm)^2 q_\mu^2)^{-2}; \quad (5)$$

$$\begin{aligned} S_x(\mathbf{k}, \mathbf{k}', \mathbf{K}) &= \frac{1}{2kk'} \left\{ \delta_{xp} \left[\left(1 + \frac{\omega}{M} + \frac{\mathbf{q}^2(1 - 2\gamma_x)}{4M^2} \right) \times \right. \right. \\ &\left. \left. \times (\varepsilon\varepsilon' + \mathbf{k}\mathbf{k}') - \frac{2}{M} \mathbf{K}(\varepsilon\mathbf{k}' + \varepsilon'\mathbf{k}) + \right. \right. \end{aligned}$$

$$\left. \left. + \frac{q_\mu^2 \mathbf{K}^2 + 4(\mathbf{k}\mathbf{K})(\mathbf{k}'\mathbf{K})}{2M^2} \right] + \gamma_x^2 \frac{4[\mathbf{k}\mathbf{k}']^2 + (q_\mu^2)^2}{4M^2} \right\} \quad (6)$$

is a dimensionless positive ($S_x(\mathbf{k}, \mathbf{k}', \mathbf{K}) \sim 1$) function of the vector arguments \mathbf{k} , \mathbf{k}' , and \mathbf{K} , which changes rather smoothly, as the kinematic parameters of electron scattering by the atomic nucleus vary. Note that the function $S_x(\mathbf{k}, \mathbf{k}', \mathbf{K})$ mainly reflects the structural features of the interaction between the relativistic electron and the quasirelativistic non-point nucleon in the McVoy–Van Hove Hamiltonian [1, 2].

The emission probability for a virtual photon $q_\mu = (\mathbf{q}, i\omega)$ at the electron vertex μ ($q_\mu = (\mathbf{q}, i\omega)$) is connected with the dimensionless function

$$P(\mathbf{k}, \mathbf{k}') \equiv P(\theta') = \frac{\mathbf{k}^2 \mathbf{k}'^2}{(q_\mu^2)^2}, \quad (7)$$

and the probability that this virtual q_μ -photon knocks out an x -nucleon from the bound xnl -state of the nucleus A to the state $|\mathbf{K}\rangle$ in the continuous spectrum of the same nucleus, with the function

$$\begin{aligned} G_{xnl}(\mathbf{q}, \mathbf{K}) &= \frac{1}{(2l + 1)(2\pi)^3} \times \\ &\times \sum_{m=-l}^{m=l} \left| \int \left(\psi_{\mathbf{K}}^{(-)*}(\mathbf{r}) \exp(i\mathbf{q}\mathbf{r}) \varphi_{xnlm}(\mathbf{r}) \right) d^3\mathbf{r} \right|^2 \end{aligned} \quad (8)$$

describing the perturbed distribution of x -nucleons over the momenta in the xnl -shell of the atomic nucleus [6, 30]. It is in functions (7) and (8) that the most important features of the processes of inelastic electron scattering by atomic nuclei, which are known as *quasireal photons* and *Coulomb (centrifugal) resonances* [18, 19, 23, 29–31], are hidden.

2. Coulomb Resonances, Quasireal Photons, and Quasidiscrete Nuclear Spectra

To clarify the role of Coulomb resonances and quasireal photons in the processes of nuclear electrodisintegration by high-energy electrons, let us consider some features inherent to the processes of inelastic high-energy electron scattering by some (medium and heavy) atomic nuclei. For this purpose, remaining in the framework of the nuclear shell model, let us append formula (2) by the definitions of the following additional quantities: the cross-section of inelastic electron scattering at a certain scattering angle θ'

and with a knockout of nucleons from the xnl -shell ($\sigma_{xnl}(\omega)|_{\theta'=\theta'_0} \equiv \sigma_{xnl}(\omega)$),

$$\sigma_{xnl}(\omega)|_{\theta'=\theta'_0} = \int d\Omega_{\mathbf{K}} \sigma_{xnl}(\mathbf{k}, \mathbf{k}', \mathbf{K})|_{\theta'=\theta'_0} \quad (9)$$

and the total cross-section of inelastic electron scattering at the same angle, which depends on the transferred energy ω ,

$$\sigma(\omega)|_{\theta'=\theta'_0} \equiv \sum_{xnl} \sigma_{xnl}(\omega)|_{\theta'=\theta'_0}. \quad (10)$$

In the case of nuclear electro-disintegration, if the interaction between the knocked out nucleons in the final state and the residual nucleus ($A - 1$) is taken into account, the cross-sections of inelastic scattering at resonance transferred energies,

$$\varepsilon_{\text{rez}} = \omega_{xnl \rightarrow xNL} = E_{xNL} + |\varepsilon_{xnl}| \equiv \omega_{[r]}, \quad (11)$$

can reach huge values [30]³. In this case, the extremely useful physical information can be obtained by calculating the excitation cross-sections of Coulomb resonances, which are determined by the cross-sections of inelastic electron scattering at the resonance energies indicated above,

$$E_{\text{rez}} \equiv \omega_{xnl \rightarrow xNL} = E_{xNL} + |\varepsilon_{xnl}|.$$

Hence, the specific excitation cross-sections of Coulomb and centrifugal resonances ($\sigma_{xnl \rightarrow xNL}^{ii}$) for inelastic electron scattering at a certain scattering angle θ' and a nucleon knockout from the xnl -shell of the atomic nucleus are determined by the formula

$$\sigma_{xnl}^{ii} = \frac{1}{N_{xnl}} \int_{\omega_{[r]} - \Delta E_s}^{\omega_{[r]} + \Delta E_s} \sigma_{xnl}(\omega) d\omega. \quad (12)$$

Note that, as a rule, σ_{xnl}^{ii} is measured in the nb/sr units. To obtain the total excitation cross-section σ_{xnl}^i of corresponding resonance, it is necessary to multiply σ_{xnl}^{ii} by Ω_{exper} , the solid angle in which inelastically scattered electrons are registered in physical experiments. We assume that $\Omega_{\text{exper}} \ll$

$\ll 1$. Formula (12) implicitly contains the inequality $\gamma_{xnl} \ll \Delta E_s$. Formula (12) also implicitly postulates that the examined resonance is isolated, i.e. the energy ΔE_s is much less than the energy interval $|\omega_{[r]} - \omega_{[r']}|$ between two neighbor Coulomb resonances registered in experiment.

Hence, in what follows, we adopt that the condition

$$\gamma_{xNL} \ll \Delta E_s \ll |\omega_{[r]} - \omega_{[r']}| \quad (13)$$

holds true, and the inequality

$$\lambda \approx \frac{m\omega}{\varepsilon\varepsilon'} \ll 1 \quad (14)$$

is satisfied. Then it is also possible to approximately determine the total excitation cross-section of Coulomb resonance, when a single proton is knocked out from the pnl -shell of the atomic nucleus at the inelastic electron scattering:

$$\begin{aligned} \sigma_{xnl \rightarrow xNL}^{ur}(\omega) &= \frac{1}{N_{xnl}} \iint_{(\Omega=4\pi)} d\Omega' \int_{\omega_{[r]} - \Delta E_s}^{\omega_{[r]} + \Delta E_s} d\omega [\sigma_{xnl}(\omega, \theta')] \approx \\ &\approx \frac{1}{N_{xnl}} \iint_{(\Omega=4\pi)} d\Omega' \int_{-\infty}^{\infty} d\omega [\sigma_{xnl}(\omega, \theta')]. \end{aligned} \quad (15)$$

The integration in Eq. (15) under conditions (13) and (14) is easy to be done [29].

The integral cross-sections σ_{xnl}^i of inelastic electron scattering at a certain scattering angle and with the knockout of protons from the xnl -shell or all (σ^i) proton and neutron shells of the considered atomic nucleus equal

$$\sigma_{xnl}^i |_{\theta'=\theta'_0} = \int_0^{\varepsilon} d\omega [\sigma_{xnl}(\omega) |_{\theta'=\theta'_0}], \quad (16)$$

$$\sigma^i |_{\theta'=\theta'_0} = \int_0^{\varepsilon} [\sigma(\omega) |_{\theta'=\theta'_0}] d\omega. \quad (17)$$

Since the occupation numbers are substantially different in different nuclear shells, the useful physical information can be obtained by analyzing the specific knockout cross-sections of single xnl -nucleons from the atomic nucleus,

$$\sigma_{xnl}^{iu} = \frac{1}{N_{xnl}} \int_0^{\varepsilon} d\omega \sigma_{xnl}(\omega) |_{\theta'=\theta'_0}. \quad (18)$$

³ Hereafter, instead of a cumbersome sequence of symbols [$xnl \rightarrow xNL$], we use a shorter and more convenient symbol [r].

Taking advantage of the properties of the function $\sigma_{xnl}(\omega, \theta')$ described earlier [30], we may assert that the integral

$$\begin{aligned} \sigma_{xnl \rightarrow xNL}^{ur}(\omega) &= \frac{1}{N_{xnl}} \int_{(\Omega=4\pi)} \int_{\omega_{[r]} - \Delta E_s}^{\omega_{[r]} + \Delta E_s} d\Omega' \int d\omega \sigma_{xnl}(\omega, \theta') = \\ &= \frac{2\pi}{N_{xnl}} \int_0^{\theta'_0} \sin \theta' d\theta' \int_{\omega_{[r]} - \Delta E_s}^{\omega_{[r]} + \Delta E_s} \sigma_{xnl}(\omega, \theta') d\omega \end{aligned} \quad (19)$$

approximately determines the lower limit for the excitation cross-section of the Coulomb pNL -resonance at the proton knockout from the pnl -shell of the atomic nucleus⁴.

A detailed analysis of the properties of the function $\sigma_{xnl}(\omega, \theta')$ depending on two kinematic variables, the energy ω transferred from the electron to the knocked out proton and the angle θ' of inelastic electron scattering, demonstrates that, in a close vicinity of the point corresponding to the resonance energy E ($\omega_{[r]} - \Delta E_s < E < \omega_{[r]} + \Delta E_s$, where $\omega_{[r]} = \omega_{xnl \rightarrow xNL}$) and the electron scattering angle $\theta' = 0$, the cross-section $\sigma_{xnl \rightarrow xNL}^{ur}(E, \theta')$ of inelastic electron scattering accompanied by the excitation of a Coulomb resonance can be approximately written in the form [30]

$$\sigma_{xnl \rightarrow xNL}(\omega, \theta') \sim \frac{B_{[r]}(\omega, \theta')}{(\theta'^2 + \lambda^2)^2 [(\omega - \omega_{[r]})^2 + \frac{\gamma_{xNL}^2}{4}]} \quad (20)$$

According to the results of calculations, the function $B_{[r]}(\omega, \theta')$ of two variables ω and θ' that enters formula (20) changes rather smoothly in a vicinity of the point ($\omega = \omega_{[r]}, \theta' = 0$). It is evident that, under those conditions, the maximum value $\sigma_{[r]}^m(\omega, \theta')$ of the inelastic electron scattering cross-section function $\sigma_{[r]}^{ur}(\omega, \theta')$ is reached at the point ($\omega = \omega_{[r]}, \theta' = 0$),

$$\begin{aligned} \sigma_{xnl \rightarrow xNL}^m &\equiv \sigma_{[r]}^m = \frac{4B_{[r]}(\omega_{[r]}, 0)}{\lambda^2 \gamma_{xNL}^2} = \\ &= \frac{4\varepsilon \varepsilon' B_{[r]}(\omega_{[r]}, 0)}{m^2 \omega^2 \gamma_{xNL}^2}. \end{aligned} \quad (21)$$

⁴ It is quite evident that, at the present stage of researches, in this and other similar cases, we do not consider exchange forces arising at the excitation of neutron (centrifugal) resonances by knocking out protons from the atomic nuclei at the inelastic high-energy electron scattering.

Expanding the function $B_{[r]}(\omega, \theta')$ in a two-dimensional Taylor series in a vicinity of the point ($\omega = \omega_{[r]}, \theta' = 0$), confining the expansion to the first term $B_{[r]} = B_{[r]}(\omega_{[r]}, 0)$, and, under the conditions given above, calculating the integral in Eq. (15) approximately (the obtained accuracy is enough to make estimations), we obtain the final result in terms of the quantities that can be calculated using the corresponding calculation program:

$$\begin{aligned} \sigma_{[r]}^u(\omega, \theta')|_{\theta'=0} &\approx \frac{1}{N_{xnl}} \int_0^{2\pi} \int_0^{\pi} d\Omega' \int_{\omega_{[r]} - \Delta E_s}^{\omega_{[r]} + \Delta E_s} d\omega \sigma_{[r]}^u(\omega, \theta') \approx \\ &\approx \frac{2\pi}{N_{xnl}} \int_0^{\theta'_0} \frac{\theta' d\theta'}{(\theta'^2 + \lambda^2)^2} \int_{\omega_{[r]} - \Delta E_s}^{\omega_{[r]} + \Delta E_s} \frac{B_{[r]} d\omega}{\left[(\omega - \omega_{[r]})^2 + \frac{\gamma_{xNL}^2}{4} \right]} \approx \\ &\approx \frac{2\pi}{N_{xnl}} \int_0^{\infty} \frac{\theta' d\theta'}{(\theta'^2 + \lambda^2)^2} \int_{-\infty}^{+\infty} \frac{B_{[r]} d\omega}{\left[(\omega - \omega_{[r]})^2 + \frac{\gamma_{xNL}^2}{4} \right]} = \\ &= \frac{2\pi^2 B_{[r]}}{(\gamma_{xNL}) \lambda^2} = \frac{\pi^2 \sigma_{[r]}^m \gamma_{[r]}}{2}. \end{aligned} \quad (22)$$

Hence, in order to obtain the excitation cross-section $\sigma_{pnl \rightarrow pNL}$ of a Coulomb resonance, i.e. to approximately integrate over the solid angle of electron scattering $d\Omega'$ and the transferred energy $d\omega$, it is necessary to use formula (22). Just formula (22) is used in this work to evaluate the approximate values of excitation cross-sections of the Coulomb pNL -resonances in the case where pnl -protons are knocked out from the pnl -shell of an atomic nucleus at the inelastic high-energy electron scattering by atomic nuclei. Note that the excitations of neutron (centrifugal) resonances in the processes with participation of quasireal photons can be neglected.

Paying attention to the important role of Coulomb resonances and their influence on the course and the interpretation of experiments aimed at studying the nuclear structure in the processes of inelastic high-energy electron scattering by nuclei, let us recall some peculiarities of the resonance structure in the quasidiscrete spectrum of atomic nuclei stemming from the properties of Coulomb resonances. First of all, we note that, according to the theory, the Coulomb resonances have to manifest themselves in the spectra of inelastically scattered electrons in the form,

as a rule, of extremely high and, simultaneously, extremely narrow peaks. Those peaks are connected with the peculiarities in the behavior of the wave function $\psi_{\mathbf{K}}^{(-)*}(\mathbf{r})$ belonging to the continuous spectrum of protons in the region of the atomic nucleus observed when the energy of protons E_p grows in the interval $0 < E_p \lesssim V_C$, where V_C is the Coulomb barrier height in the atomic nucleus⁵. The theory also asserts that, in real experiments, Coulomb resonances should have finite, rather low heights [31]. However, under certain conditions, those heights can even exceed the height of the quasielastic peak [30, 31]. It is worth noting the universal character of this phenomenon. Theoretical calculations demonstrate that Coulomb resonances reveal themselves in the spectra of inelastic electron scattering by almost all ($A \gtrsim 7$) atomic nuclei and under various kinematic conditions of scattering (the electron scattering angle θ' and the initial energy of scattered electrons ε).

Note that the soundest contribution of Coulomb resonances to the theoretical physics is, undoubtedly, the standard interpretation of quasidecrete spectrum of atomic nuclei and other quantum-mechanical systems (the wave function, the exact and approximated quantum numbers, and so forth). It was Coulomb resonances that opened a way to interpret the quantum-mechanical transitions of atomic nuclei from discrete states to states in the quasidecrete spectrum (as well as from quasidecrete states to another quasidecrete and discrete ones) on the basis of standard procedures of the quantum-mechanical theory [29–31]. Moreover, it was Coulomb resonances that refuted the doubts [35] about the correctness of the method of complex energies developed by J.J. Thomson and applied by G. Gamov, while interpreting the α -decay of heavy atomic nuclei [29–31].

We have also to note that it is Coulomb resonances that allow the well-known electro-nuclear phenomenon of giant dipole resonance to be interpreted in the framework of the nuclear shell model [18, 31]. Undoubtedly, this is also an important achieve-

ment of Coulomb resonances, which allows the interpretation of giant dipole resonance in the framework of the nuclear shell model to be considerably simplified and, at least, an alternative to the known interpretation of this phenomenon in the Migdal–Goldhaber–Teller theory [32] to be proposed.

Of keen interest at the modern stage of researches is the study and the interpretation of Coulomb resonances and their interaction with quasireal photons from the viewpoint of the influence of those phenomena on the dynamics of the knockout reaction of x -nucleons (protons [$A(e, e'p)A-1; x=p$] and neutrons [$A(e, e'n)A-1; x=n$]) from different shells of atomic nuclei at the inelastic high-energy electron scattering by nuclei [18, 29–31]. Nevertheless, we should note that, despite the indicated local progress in the theory of the phenomenon concerned, the properties of Coulomb resonances and their probable influence on the course of various nuclear processes still remain a poorly studied area both in the theoretical physics in general and in the theoretical and experimental nuclear physics in particular.

Unlike Coulomb resonances, quasireal photons are an exclusively quantum electrodynamic phenomenon (Feynman's diagram technique), which accompanies the processes of inelastic scattering of relativistic electrons by hadrons. For this reason, quasireal photons can interact, e.g., with the aforesaid Coulomb resonances only in the processes of inelastic scattering of charged leptons (electrons, positrons, muons) by atomic nuclei. Note also that, in the quantum-mechanical aspect, the properties of quasireal photons emitted by electrons near an atomic nucleus are rather similar to those of real photons. That is why the processes of inelastic electron scattering by atomic nuclei at extremely small angles ($\theta' \lll \frac{m\omega}{\varepsilon\varepsilon'}$) can be efficiently used to study the giant dipole resonance phenomenon [9, 18, 19, 23, 29, 31].

It is worth to note that the role of Coulomb resonances in the theoretical nuclear physics, as well as in the general theoretical physics, is not reduced to the emergence of a peak in the cross-sections of inelastic high-energy electron scattering by nuclei. Coulomb resonances are an inherent attribute of the nuclear shell model since the moment of their appearance there, as well as a substantial extension of this model to the continuous spectrum [30, 31]. Therefore, they can affect the theoretical interpretation and the course of a lot of various nuclear processes. At the

⁵ It is pertinent to note that the presence of a Coulomb barrier (or a barrier with another shape) is not a mandatory condition for the function $\psi_{\mathbf{K}}^{(-)*}(r)$ in the continuous spectrum to have a resonance structure. Using the method proposed in works [18, 19, 23], it is easy to find, e.g., that, theoretically, there can exist the so-called antibarrier resonances. However, the properties of the latter are a little different in comparison with those of Coulomb resonances.

same time, the inelastic scattering of high-energy electrons by nuclei is only one of the most convenient platforms for the illustration of specific peculiarities (both theoretical and experimental) of the aforementioned Coulomb resonances.

3. Coulomb and Centrifugal Resonances in the jj -Shell Model of Atomic Nuclei

It is well known that, among nuclear shell models, it is undoubtedly the shell model with jj -coupling that describes the experiment rather successfully. For this reason, let us briefly consider the issue concerning the determination of the basic characteristics of Coulomb resonances in the shell model with jj -coupling⁶.

First of all, we note that the calculations of quasidecrete nuclear spectra in the shell models with LS - and jj -coupling are almost identical. They are carried out with the use of the following procedures in the case of jj -coupling [18, 19, 30]. At the first stage, we solve the radial Schrödinger equation

$$\frac{d^2 Z_{Klj}(r)}{dr^2} + [2m(E - V_{xlj}(r))] Z_{Klj}(r) = 0, \quad (23)$$

where the spin-orbit interaction of a nucleon in the atomic nucleus is taken into account. The potential energy $V_{xlj}(r)$ in Eq. (23) is a sum of four terms,

$$V_{xlj}(r) = V_{xWS}(r) + V_C(r) + \frac{l(l+1)}{2Mr^2} + V_{ls}(r),$$

where

$$V_{xWS}(r) = -\frac{V_{0Ax}}{1 + \exp\left(\frac{r-R}{a}\right)} \approx -\frac{V_{0Ax}\Theta(b-r)}{1 + \exp\left(\frac{r-R}{a}\right)}, \quad (V_{0Ax} \equiv V_{0x} > 0), \quad (24)$$

$$V_C(r) = \left[\frac{(Z-1)e^2}{R} \left(\frac{3}{2} - \frac{r^2}{2R^2} \right) \Theta(R-r) + \frac{(Z-1)e^2}{r} \Theta(r-R) \right]; \quad (25)$$

$$V_{ls}(r) = \lambda \left[(l + j_l^* - 1) \times (l + j_l^* + 1) - l(l+1) \right] \frac{2dV_{xWS}}{d(r^2)}. \quad (26)$$

⁶ The LS -coupling is a variant of the jj -coupling in the case where the spin-orbit forces can be neglected (the parameter λ governing the magnitude of spin-orbit forces equals zero: $\lambda = 0$ in Eq. (26)).

In formulas (24)–(26), the following notation is used:

$$\Theta(x) = (1 - \delta_{x0}) \frac{x + |x|}{2x} + \frac{1}{2} \delta_{x0}$$

is the Heaviside unit step function; $b \approx r_0 \sqrt[3]{A} + 18a$; V_{0Ax} , a , and $R = r_0 \sqrt[3]{A}$ are the parameters of shell potential in the Woods–Saxon form;

$$j_l^* = (j + \frac{1}{2} - l) = \begin{cases} 1, & j = l + \frac{1}{2}; \\ 0, & j = l - \frac{1}{2}; \end{cases} \quad (27)$$

is the quantum number of the mutual spin and orbital moment orientation: $j_l^* = 1$, if the spin and the orbital moment are parallel to each other ($\mathbf{1} \uparrow \uparrow \mathbf{s}$), and 0, if they are antiparallel ($\mathbf{1} \uparrow \downarrow \mathbf{s}$).

At the next stage, we match the internal and external (asymptotic) solutions of the radial Schrödinger equation (23) and determine the energy E_{xNL} and other basic characteristics (γ_{xNL} and A_{xNL}) of Coulomb (and centrifugal, i.e. neutron) resonances,

$$\begin{cases} \left. \frac{\left(\frac{dZ_{K[r]LJ}(r)}{dr} \right)}{Z_{K[r]LJ}(r)} \right|_{r=b} = \left. \frac{\left(\frac{dG_L(\eta, K[r]r)}{dr} \right)}{G_L(\eta, K[r]r)} \right|_{r=b}; \\ \frac{\gamma_{NLJ}^r}{2} = \frac{w_{FZ}^{LJ}(E)}{\left(\frac{dw_{FZ}^{LJ}(E)}{dE} \right)} \Big|_{E=E_{NLJ}^r}; \\ A_{NLJ}^{(-)}(E_{NLJ}^r) = \frac{-i}{w_{FZ}^{LJ}(E_{NLJ}^r)}; \end{cases} \quad (28)$$

Those equalities comprise the initial formulas for the determination of basic characteristics (E_{NLJ}^r , γ_{NLJ}^r , and $A_{NLJ}^{(-)}$) of Coulomb and centrifugal resonances in the nuclear shell model with jj -coupling. A new quantity introduced in Eq. (28), w_{FZ}^x , is the Wronskian of the functions $F_x(r)$ and $Z_x(r)$, i.e.

$$w_{FZ}^x = \frac{dF_x(r)}{dr} Z_x(r) - \frac{dZ_x(r)}{dr} F_x(r). \quad (29)$$

In Tables 1 to 3, the parameters of the quasidecrete spectra of the ^{119}Sn atomic nucleus obtained in the jj - ($\lambda = 0.25 \text{ fm}^2$) and LS -shell models are listed. The corresponding calculations were carried out for the following parameters of the Woods–Saxon

Table 1. Basic physical parameters
[E_{xNLJ^*} (MeV), γ_{xNLJ^*} , and A_{xNLJ^*}]
of quasidecrete spectra (Coulomb and centrifugal
resonances) of ^{119}Sn nucleus ($V_{0p} = 58.6$ MeV,
 $V_{0n} = 44.8$ MeV, and $\lambda = 0.25$ fm 2) calculated
taking the spin-orbit interaction into account

$xNLJ^*$	E_{xNLJ}	A_{xNLJ}	A_{xnlj}	γ_{xNLJ}
$n150$	0.4569	1.762×10^3	0.6351	8.003×10^{-7}
$n161$	3.800	33.40	0.631	6.358×10^{-3}
$p231$	3.824	1.600×10^2	0.526	1.927×10^{-4}
$p150$	3.865	3.344×10^3	0.665	7.079×10^{-7}
$p311$	5.938	4.321	0.403	0.2
$p161$	6.321	4.248×10^2	0.667	5.658×10^{-5}
$p230$	6.931	9.620	0.491	6.308×10^{-2}
$n160$	10.13	3.957	0.592	0.675
$n171$	12.27	4.421	0.601	0.612
$p160$	14.66	11.12	0.638	0.116
$p171$	15.49	14.58	0.651	0.072
$p181$	24.86	4.911	0.632	0.773

Table 2. Basic physical parameters
[E_{xNLJ} (MeV), γ_{xNLJ} (MeV), and A_{xNLJ}]
of quasidecrete spectra (Coulomb and centrifugal
resonances) of ^{119}Sn nucleus ($V_{0p} = 62$ MeV
and $V_{0n} = 50$ MeV) calculated for the absence
of spin-orbit interaction (the LS -coupling, $\lambda = 0.0$)

xNL	E_{xNL}	A_{xNL}	A_{xnl}	γ_{xNL}
$pnl = p15$	$E_{p15} = -2.263$
$p23$	2.941	891.23	0.5323	5.58×10^{-6}
$n16$	3.534	46.511	0.6388	3.23×10^{-3}
$p31$	4.525	13.642	0.4316	1.95×10^{-2}
$p16$	7.918	147.73	0.6655	5.20×10^{-4}
$n17$	13.15	4.2047	0.6024	0.703
$p17$	18.25	8.6780	0.6375	0.212

shell potential: ($V_{0p} = 58.6$ MeV, $V_{0n} = 44.8$ MeV) and ($V_{0p} = 62.0$ MeV, $V_{0n} = 50.0$ MeV). The results of similar calculations are systematized in Tables 4 and 5 for the case of the heavier atomic nucleus, ^{181}Ta ⁷. Brief conclusions that result from the comparison of results in the quoted tables are as follows. As the depth of shell potential increases, the

⁷ In all tables presented in this work, the energy quantities E_{xNLJ^*} and γ_{xNLJ^*} are expressed in terms of megaelectronvolts, A_{xNLJ^*} is a dimensionless quantity, and the amplitude A_{xnlj} is expressed in terms of the fm $^{-2}$ units.

Table 3. Basic physical parameters
[E_{xNLJ} (MeV), γ_{xNLJ} (MeV), and A_{xNLJ}]
of quasidecrete spectra (Coulomb and centrifugal
resonances) of ^{119}Sn nucleus ($V_{0p} = 58.6$ MeV
and $V_{0n} = 44.8$ MeV) calculated for the absence
of spin-orbit interaction (the LS -coupling, $\lambda = 0.0$)

NLx	E_{xNL}	A_{xNL}	A_{xnl}	γ_{xNL}
$15p$	0.4677	4.143×10^{13}	0.6648	1.605×10^{-27}
$23n$	0.5941	9.756	0.4414	1.4239×10^{-2}
$23p$	5.161	33.37	0.5128	4.892×10^{-3}
$31p$	6.263	3.616	0.3971	0.2893
$16n$	6.768	8.374	0.6050	0.1252
$16p$	10.29	40.17	0.6534	7.741×10^{-3}
$17p$	20.27	5.779	0.6225	0.4850

quasidecrete spectrum of the nucleus becomes, as a rule, somewhat more powerful. This phenomenon manifests itself more pronouncedly in the case of the jj -shell model.

Note that the main conclusions of this work depend on the accuracy of numerical calculations in the applied software programs. It is desirable to monitor, in that or another way, all program units used in numerical calculations. Here are some examples of such a monitoring. At a certain stage of numerical calculations, when Coulomb resonances of small energies were studied, there emerged a necessity to determine the characteristics of proton quasidecrete states in order to improve the calculation accuracy for the Coulomb functions. It is rather simple to enhance the capabilities of algorithms proposed for this procedure in work [38]. However, it is impossible to check the accuracy of the results obtained in the framework of this procedure on the basis of the results tabulated in work [38]. To be convinced of the efficiency of the used algorithms, the following empirical trick was applied. For the Coulomb functions calculated with the use of the advanced technique, the Wronskian

$$W(F, G) = F'(\rho, \eta)G(\rho, \eta) - G'(\rho, \eta)F(\rho, \eta) = 1 \pm \delta \quad (30)$$

was determined. For “typical” values of parameters ρ and η ($1 \lesssim (\rho, \eta) \lesssim 10$), the calculation error equaled $\delta \lesssim 10^{-14} \div 10^{-13}$. For “nontypical” parameter values ($\rho \lesssim 1$ and $\eta \sim 100$), the calculation error substantially grew to $\delta \lesssim 10^{-10} \div 10^{-9}$. The result obtained in such a manner testifies, without

additional researches, to the relative efficiency of the applied technique.

Here is another example. It is clear that the efficiency of a calculation procedure considerably depends on the successful application of the Numerov method to the solution of radial Schrödinger equations of type (23). However, even after an acquaintance with the analyses, as much detailed as possible, concerning the application of this method to the solution of the quantum-mechanical radial equations [12], the authors still have a wide opportunity to take the initiative, while interpreting those or other specific issues of this application. First of all, this remark is valid for the application of the Numerov method in the interval $r \ll r_0$. To be convinced of the efficiency of the applied numerical methods, while obtaining the starting solution of the radial Schrödinger equations, one can use the following trick, as an example. It is well known that the eigenvalues of the Sturm–Liouville problem in the case of Legendre or Gegenbauer polynomials can be determined theoretically rather easily [14]. For instance, the Sturm–Liouville problem for the Gegenbauer polynomials is defined by the differential equation

$$\frac{1}{\sin^2 \alpha} \frac{d}{d\alpha} \sin^2 \alpha \frac{dU}{d\alpha} + \left[\varepsilon - \frac{l(l+1)}{\sin^2 \alpha} \right] U(\alpha) = 0. \quad (31)$$

At small values of variable α , this equation is almost identical to the radial Schrödinger equation [14]. The solution of problem (31) is known: $\varepsilon = N(N+2)$ [14]. Reproducing this solution with the help of numerical calculations taking advantage of the procedures elaborated by us for the solution of Eq. (31) ($\varepsilon = N(N+2) \pm \delta$) and evaluating the accuracy of the obtained solution ($|\delta| \leq 10^{-10}$), we may be convinced of the relative efficiency of the engaged programming techniques to apply the Numerov method to the solution of the radial Schrödinger equation.

Comparing the data quoted above, we should point out, first of all, a substantial growth in the number of quasidiscrete states (as well as the bound states of nucleons) in the case of the jj -shell model (in comparison with the LS -shell model, see Tables 1 and 4). In practice, this fact gives rise to a considerable increase in the number of resonance points in the dependence of $\sigma(\omega, \theta')$ on the transferred energy ω . The latter circumstance brings about additional and often not ordinary technological difficulties even in the case of medium atomic nuclei. Considering the al-

Table 4. Basic physical parameters of quasidiscrete spectra (Coulomb and centrifugal resonances) of ^{181}Ta nucleus ($V_{0p} = 62$ MeV, $V_{0n} = 50$ MeV, and $\lambda = 0.25$ fm 2) calculated taking into account the spin-orbit interaction

NLJ^*x	E_{xNLJ}	A_{xNLJ}	A_{xnlj}	γ_{xNLJ}
321n	-1.585
401n	-0.8508
311p	-0.2144
230p	-9.719×10^{-2}
310p	1.250	3.573×10^8	0.4785	1.828×10^{-17}
251n	3.187	5.504	0.4670	0.1204
171p	3.695	6.429×10^5	0.6716	1.912×10^{-11}
241p	4.033	4.355×10^3	0.5447	2.863×10^{-7}
160p	4.698	3.301×10^4	0.6669	8.062×10^{-9}
181n	5.141	97.08	0.6528	9.3460×10^{-4}
170n	6.421	22.20	0.6361	1.9010×10^{-2}
321p	7.545	10.67	0.4445	4.3796×10^{-2}
240p	9.064	21.67	0.5200	1.5825×10^{-2}
320p	9.734	3.665	0.4166	0.3845
181p	11.67	241.6	0.6743	2.426×10^{-4}
251p	11.69	9.652	0.5124	8.861×10^{-2}
191n	13.26	10.44	0.6356	0.1242
170p	14.83	41.76	0.6620	8.823×10^{-3}
180n	16.34	4.163	0.6123	0.8211
191p	19.99	26.50	0.6691	2.602×10^{-2}
1(10)1n	21.62	4.618	0.6235	0.8224
180p	25.40	7.352	0.6414	0.3607
1(10)1p	28.59	9.253	0.6572	0.2478

Table 5. Quasidiscrete spectrum (Coulomb and centrifugal resonances: E_{xNL} , A_{xNL} , γ_{xNL}) of ^{181}Ta nucleus. The Woods–Saxon potential parameters: $V_{0p} = 59.222$ MeV and $V_{0n} = 52.3405$ MeV (the LS -coupling)

NLx	E_{xNL}	A_{xNL}	A_{xnl}	γ_{xNL}
17n	6.701×10^{-3}	2.5988×10^{11}	0.6509	4.6801×10^{-24}
23p	2.296×10^{-2}	2.5128×10^{97}	0.5420	6.4260×10^{-196}
31p	2.339	8.3725×10^4	0.4730	4.4478×10^{-10}
16p	2.590	8.0588×10^6	0.6572	9.7548×10^{-14}
25n	3.931	3.8596	0.4533	0.2603
24p	8.190	31.96	0.5201	6.9120×10^{-3}
18n	9.070	16.92	0.6325	3.8514×10^{-2}
17p	11.30	1.312×10^2	0.6553	7.6379×10^{-4}
19n	18.24	4.540	0.6077	0.7211
18p	20.34	13.14	0.6387	9.7596×10^{-2}

most complete absence of detailed experimental data in the given domain of researches and the preliminary character of calculations in this work, further conclusions should be made, and qualitative researches should be carried out in the framework of the simplified shell model with LS -coupling. Note that, in this case, the main components of theoretical conclusions in this work will not undergo substantial modifications. Another important conclusion is expedient to be drawn: discrete and quasidecrete energy levels are interchangeable, when the potential parameters in the shell model are varied. In other words, a quasidecrete level (or its part emerging when this level is split) can transform sometimes into a bound state even at relatively small, almost unobservable, and even insignificant variations of the potential parameters. *Vice versa*, for the opposite change of the shell potential parameters, the bound state of a nucleon in the atomic nucleus can transform into a quasidecrete state of this nucleon in the atomic nucleus.

As an example, let us consider a change of the status of the quasidecrete level $p15$. In the case $V_{0p} = 58.6$ MeV (see Table 3), level $p15$ is a low-lying resonance state of the nucleus ^{119}Sn . At the same time, in the case $V_{0p} = 62$ MeV, state $p15$ is a bound proton state of the same nucleus with the binding energy $\varepsilon_{p15} = -2.263$ MeV indicated in Table 2. Similar examples for Coulomb and centrifugal neutron resonances can be given as many as is desired.

Note again that even almost indiscernible modifications in the shell potential parameters turn out sometimes sufficient for a high-lying discrete level or a low-lying quasidecrete level to change its status. Such quantum-mechanical states (discrete and quasidecrete ones) obtained at arbitrary modifications of the potential in the shell model will be referred to as cognate.

The indicated factor changing the status of the shell energy level turns out, in this case, a crucial provoking issue that evidently verifies and explicitly declares the common origin of discrete and quasidecrete spectra of atomic nuclei in the framework of the nuclear shell model. Below, the shell model together with a set of quasidecrete energy levels will be referred to as the extended shell model of atomic nuclei.

In connection with the aforementioned possibility for the levels in the discrete and quasidecrete spectra to change their status as the potential parameters vary and in order to correctly interpret the ex-

perimental results (e.g., to specify the parameters of the Woods–Saxon potential), the comparison of cross-sections at the inelastic high-energy electron scattering by nuclei accompanied by the excitation of cognate levels in the discrete and quasidecrete spectra becomes of vital importance in the nuclear shell model. For the sake of such a comparison, the tables calculated for the quasidecrete spectra of nuclei include the basic and auxiliary information about the amplitudes A_{xNL} and A_{xnl} of the wave functions for the low-lying quasidecrete and high-lying bound cognate (with the same quantum numbers NL) states (practically, at the same parameters of the shell potential), which was taken from works [6, 30]. The amplitudes were normalized according to the formulas

$$A_{xNL} = \frac{R_{KL}(r_{1m})}{|i[F_L(Kb)R'_{KL}(b) - F'_L(Kb)R_{KL}(b)]|}; \quad (32)$$

$$A_{xnl} = \frac{R_{nl}(r_{1m})}{\int_0^\infty [R_{nl}(r)]^2 r^2 dr}; \quad (33)$$

where r_{1m} is a point, where the functions $R_{KL}(r)$ and $R_{nl}(r)$ have the first maximum. Note that the proportionality between the radial components $R_{KL}(r)$ and $R_{nl}(r)$ takes place in this case with a high accuracy at any point r , where $R_{nl}(r) \neq 0$:

$$\begin{aligned} \frac{R_{KL}(r)}{R_{nL}(r)} &\approx \frac{|A_{xNL}|}{|A_{xnl}|} \approx \\ &\approx \frac{\sqrt{\int_0^b [R_{nl}(r)]^2 r^2 dr}}{|i[F_L(Kb)R'_{KL}(b) - F'_L(Kb)R_{KL}(b)]|}, \quad r \lesssim r_0. \end{aligned} \quad (34)$$

With the help of the information given above, it is easy to find the ratio between the excitation cross-sections of a high-lying discrete state of the atomic nucleus, $\sigma_{n_x l_x \rightarrow n_l l}^u$ [3], and a low-lying (cognate) quasidecrete state, $\sigma_{n_x l_x \rightarrow N_L L}^u$ (here, $n_l = N_L$ and $l = L$).

Hence, the facts presented above testify that the shell model of a nucleus can be appended by the quasidecrete spectrum of this nucleus, i.e. the limits of nuclear shells can be expanded with the help of specific one-particle states of nucleons in the interval of positive energies. Note that the potential parameters

r_0 and a were constant in all calculations of this work: $r_0 = 1.24$ fm and $a = 0.55$ fm. It will also be recalled that the quantum numbers E_{xNL} , γ_{xNL} , and A_{xNL} of nucleon states in the quasisdiscrete spectrum of the atomic nucleus are approximate. An exact quantum number of the problem is the momentum vector for the knocked out proton, \mathbf{K}_p .

At last, the data in Table 6 illustrate, rather completely, the dependences of the basic characteristics of the Coulomb resonance with the quantum numbers $pNL = p15$ on the parameter V_{0p} in the Woods–Saxon potential $V_{pWS}(r)$. It follows that, in some regions, the variation of this parameter in the sixth (!) digit of mantissa – e.g., $0.5920222 \times 10^2 \rightarrow 0.5920200 \times 10^2$ – results in a relatively insignificant growth of the Coulomb resonance energy, but simultaneously its half-width becomes six (!) orders of magnitude larger.

4. Inelastic High-Energy Electron Scattering at Large Scattering Angles

In this work, we analyze and compare the excitation cross-sections of nuclear Coulomb resonances, when electrons are scattered at large ($\theta' = 60^\circ$) and small ($\theta' = 10^{-12}$ deg) angles. The excitation cross-sections of Coulomb (protons) and centrifugal (neutrons) resonances at the inelastic electron scattering at the angle $\theta' = 60^\circ$ are quoted in Tables 7 and 8, whereas Table 9 contains the excitation cross-sections of Coulomb (only protons) resonances for the inelastic scattering of electrons at the angle $\theta' = 10^{-12}$ deg $\lll \frac{m\omega}{\varepsilon\varepsilon'}$.

To illustrate each of the statements made above, let us consider, e.g., the scattering of high-energy electrons ($\varepsilon = 500$ MeV and $\theta' = 60^\circ$) [11] by the atomic nucleus $^{119}_{50}\text{Sn}$. The parameters of the Woods–Saxon potential were so chosen that 50 protons and 69 neutrons of this nucleus could be effectively arranged in the bound states calculated with the use of the chosen shell potential⁸.

⁸ Note that the choice of parameters for the Woods–Saxon potential on the basis of experimental data of the same type is an ambiguous operation. Using the results of separate physical experiments, we can only indicate often the limits, within which the shell potential parameters change. In these and all further calculations, the parameters of the Woods–Saxon potential were constant: $a = 0.55$ fm and $r_0 = 1.24$ fm. The required variations in the structure of nuclear spectra were made by changing the parameter V_{0x} .

Table 6. Dependence of the basic parameters (E_{xNL} , A_{xNL} , γ_{xNL}) of the resonance $15p$ of the ^{199}Sn nucleus on the energy E_{xNL} of a quasisdiscrete level of this Coulomb resonance (or the shell potential depth V_{0p})

xnl	E_{p15}	A_{p15}	A_{p15}	γ_{p15}	V_{0p}
$p15$	4.178×10^{-3}	1.828×10^{161}	0.6660	9.881×10^{-324}	59.20242
$p15$	4.193×10^{-3}	9.151×10^{160}	0.6660	2.964×10^{-323}	59.20240
$p15$	4.270×10^{-3}	3.043×10^{159}	0.6660	2.853×10^{-320}	59.20230
$p15$	4.332×10^{-3}	2.135×10^{158}	0.6660	5.839×10^{-318}	59.20222
$p15$	4.501×10^{-3}	1.901×10^{155}	0.6660	7.503×10^{-312}	59.20200
$p15$	5.272×10^{-3}	2.106×10^{143}	0.6660	6.616×10^{-288}	59.20100
$p15$	5.349×10^{-3}	1.872×10^{142}	0.6660	8.434×10^{-286}	59.20090
$p15$	5.658×10^{-3}	1.928×10^{138}	0.6660	8.184×10^{-278}	59.20050
$p15$	6.005×10^{-3}	1.485×10^{134}	0.6660	1.420×10^{-269}	59.20005
$p15$	3.687×10^{-2}	9.993×10^{52}	0.6659	7.770×10^{-107}	59.16000
$p15$	5.228×10^{-2}	9.959×10^{34}	0.6658	3.426×10^{-89}	59.14000
$p15$	6.770×10^{-2}	4.364×10^{38}	0.6658	5.518×10^{-78}	59.12000
$p15$	0.5444	3.102×10^{12}	0.6646	3.087×10^{-25}	58.50000
$p15$	0.9274	1.403×10^{09}	0.6657	1.962×10^{-18}	58.00000
$p15$	1.690	1.900×10^{06}	0.6614	1.436×10^{-12}	57.00000
$p15$	2.822	2.436×10^{04}	0.6579	1.117×10^{-8}	55.50000

It is also worth noting that the quasisdiscrete levels with the energy close to the energy V_C of the nuclear Coulomb barrier have rather a wide halfwidth γ_{xNL} . An example of such a quasisdiscrete state is the state with the quantum numbers $xNL = p17$. Although the inequality $\gamma_{xNL} \ll E_{xNL}$ still holds true for such states, the strong inequality $\gamma_{xNL} \lll \lll \Delta E_s \ll \omega_{xnl \rightarrow xNL}$ is no more satisfied. Therefore, the accuracy of calculations carried out by formula (22) for such emerging high-lying quasisdiscrete levels becomes considerably lower. For example, the specific excitation cross-sections of such resonances calculated with the use of the same formula (22) turn out overestimated. Hence, calculations for such quasisdiscrete states have a preliminary evaluating character.

Looking through the specific excitation cross-section values for Coulomb and centrifugal resonances at the electron scattering by the large angle $\theta' = 60^\circ$ presented in Tables 7 and 8, attention is attracted to their small magnitudes and an insignificant growth for protons and neutrons in external shells, as well as to a similar insignificant growth of the specific excitation cross-sections of resonances with the resonance quantum number L at a con-

Table 7. Specific excitation cross-sections $\sigma_{pnl \rightarrow pNL}^{ur}$ (in nb/sr units) of proton Coulomb resonances at the inelastic electron scattering by the ^{119}Sn nucleus at the angle $\theta' = 60^\circ$. The depth parameter of the Woods–Saxon potential, $V_{0p} = 58.6$ MeV. The energy of bombarding electrons $\varepsilon = 500$ MeV

$\sigma_{pnl \rightarrow pNL}^{ur}$					
Quantum numbers pNL of Coulomb					
$[pnl] \downarrow$	15	23	31	16	17
10	4.770×10^{-3}	7.591×10^{-3}	4.3712×10^{-3}	5.1680×10^{-3}	0.1063
11	1.194×10^{-2}	1.259×10^{-2}	3.1082×10^{-3}	0.1324	0.4333
12	0.1120	0.1574	0.0690	0.4047	0.9243
20	0.1948	0.3064	0.1381	0.3564	0.3925
13	0.3379	0.3628	0.1374	0.8411	1.4070
21	0.3815	0.7533	0.4227	0.3730	0.4695
14	0.6688	0.4884	0.0942	1.2521	1.7340

Table 8. Specific excitation cross-sections $\sigma_{nl(n) \rightarrow NL(n)}^{ur}$ (in nb/sr units) of neutron (centrifugal) resonances, the excitation energies of those centrifugal resonances (in MeV units), and the integral scattering cross-sections $\sigma_{[r]}^{i(n)}$ (in nb/sr units) at the inelastic electron scattering by the ^{119}Sn nucleus at the angle $\theta' = 60^\circ$. The depth parameter of the Woods–Saxon potential, $V_{0p} = 44.8$ MeV. The notation $[r] \equiv nl(n) \rightarrow NL(n)$ is used. The energy of bombarding electrons $\varepsilon = 500$ MeV

Bound states	Specific cross-sections of neutron NLn -resonances (nb/sr), the excitation energies of those resonances $\omega_{[[r]]}$ (MeV), the integral scattering cross-sections $\sigma_{[[r]]}^{in}$ (nb/sr)					
	$nl(n)$	$23n$	$\omega_{nl(n) \rightarrow 23n}$	$16n$	$\omega_{nl(n) \rightarrow 16n}$	$\sigma_{[r]}^{i(d)}$ (nb/sr)
10	4.133×10^{-4}	39.70	9.222×10^{-4}	45.88	27.44	29.67
11	1.488×10^{-3}	34.17	1.895×10^{-2}	40.35	27.57	29.70
12	1.910×10^{-2}	27.55	6.366×10^{-2}	33.72	27.73	29.86
20	3.923×10^{-2}	25.23	6.326×10^{-2}	31.41	27.80	29.89
13	4.971×10^{-2}	20.01	0.141	26.18	27.83	30.13
21	0.107	16.69	7.870×10^{-2}	22.86	27.81	30.40
14	7.377×10^{-2}	11.71	0.223	17.88	28.18	30.17
22	0.141	8.01	0.109	14.18	27.94	29.95
30	0.150	6.93	1.099×10^{-2}	13.10	28.17	29.71

stant quantum number $N \equiv N_L$. Let us also pay attention to the almost constant integral scattering cross-section calculated with regard for the rescattering in the final state (Table 8, column 5) and in the plane-wave approximation (column 6) in the case of the neutron knockout from all neutron shells of the ^{119}Sn nucleus. In other words, under the conditions of the analyzed kinematics, the integral scattering ability of a nucleon (both a proton [30] and a neutron) practically does not depend on the quantum numbers of the shell, in which the nuclear nucleon moves.

Note also that, at large angles of the inelastic high-energy electron scattering, the specific excitation cross-sections of protons and neutrons are of the same order of magnitude. The theory predicts that one may not omit the neutron component of nuclei in experiments on the inelastic scattering of high-energy electrons at large angles. However, the same theory demonstrates that, at the inelastic scattering of electrons at extremely small angles, the neutron component of nuclei can be neglected. Some specific features of the “0-0”-scattering of high-energy electrons by the ^{119}Sn nucleus are considered in the next section.

5. Inelastic Scattering of Electrons at Extremely Small Angles. Giant Dipole Resonance Phenomenon

To consider whether such a well-known phenomenon in nuclear physics as the giant dipole resonance can be interpreted in the framework of the nuclear shell model, let us analyze the specific features of the inelastic scattering of electrons at extremely small angles, $\theta' = 10^{-12}$ deg $\lll \frac{m\omega}{\varepsilon\varepsilon'}$. First of all, we note that, in order to calculate various cross-sections of inelastic high-energy electron scattering by atomic nuclei, we must be able to calculate the overlap integral [31]

$$I(\mathbf{K}, \mathbf{q}, nlm) = \iiint_{-\infty}^{+\infty} d\mathbf{r} \psi_{\mathbf{K}}^{(-)*}(\mathbf{r}) \exp(i\mathbf{q}\mathbf{r}) \varphi_{nlm}(\mathbf{r}). \quad (35)$$

with a sufficient accuracy. In this work, we applied the following calculation procedure. Using the standard expansions of the functions $\psi_{\mathbf{K}}^{(-)*}(\mathbf{r})$ and $\exp(i\mathbf{q}\mathbf{r})$ in the series in spherical functions [31] and the values of the integral of three spherical functions [36], we can write down

$$\begin{aligned} I(\mathbf{K}, \mathbf{q}, nlm) &= (4\pi)^2 \times \\ &\times \sum_{l_k=0}^{l_k=\infty} \sum_{m_k=-l_k}^{m_k=+l_k} \sum_{l_q=0}^{l_q=\infty} \sum_{m_q=-l_q}^{m_q=+l_q} \sqrt{\frac{(2l_q+1)(2l+1)}{4\pi(2l_k+1)}} \times \\ &\times (i)^{l_q+l_k} (-1)^{l_k} \langle l_q 0 l 0 | l_k 0 \rangle \langle l_q 0 l m | l_k m \rangle \times \\ &\times B_{l_k l_q}(K, q, nl) Y_m^{l_k*} \left(\frac{\mathbf{K}}{K} \right) Y_m^{l_q} \left(\frac{\mathbf{q}}{q} \right), \end{aligned} \quad (36)$$

where

$$\begin{aligned} B_{l_k l_q}(K, q, nl) &= \int_0^b [R_{K l_k}(r) j_{l_q}(qr) R_{nl}(r) r^2 dr] / \\ &/ [(G_{l_k}(Kb) R'_{l_k}(b) - G'_{l_k}(Kb) R_{l_k}(b))] + \\ &+ i(F_{l_k}(Kb) R'_{l_k}(b) - F'_{l_k}(Kb) R_{l_k}(b)). \end{aligned} \quad (37)$$

Using the known formula of the theory of spherical functions [36],

$$Y_m^l(\nu) |_{\nu \parallel \mathbf{e}_z} = \delta_{m0} \sqrt{\frac{(2l+1)}{4\pi}}, \quad (38)$$

and the properties of Clebsch–Gordan coefficients [36], equality (36) can be presented in the coordinate system, where $\mathbf{e}_z \parallel \mathbf{q}$, in the form

$$\begin{aligned} I(\mathbf{K}, q, nlm) &= (4\pi) \sum_{l_k=0}^{l_k=\infty} \sum_{k=0}^{k=l} (2l_q+1) \times \\ &\times \sqrt{\frac{(2l+1)}{(2l_k+1)}} (i)^{l_q+l_k} (-1)^{l_k} \langle (l_k-l+2k) 0 l 0 | l_k 0 \rangle \times \\ &\times \langle (l_k-l+2k) l m | l_k m \rangle B_{l_k l_q}(K, q, nl) Y_m^{l_k*}(\nu_{\mathbf{K}}) \end{aligned} \quad (39)$$

where

$$\nu_k = \left(\frac{\mathbf{K}}{K} \right). \quad (40)$$

At last, the function $G_{xNL}(\mathbf{q}, \mathbf{K})$ describing the perturbed distribution of nucleons over the momenta and defined in Eq. (8) can be expressed in the form⁹

$$\begin{aligned} G_{xnl}(\mathbf{q}, \mathbf{K}) &= \frac{1}{(2l+1)(2\pi)^3} \times \\ &\times \sum_{m=-l}^{m=l} \left| \int (\psi_{\mathbf{K}}^{(-)*}(\mathbf{r}) \exp(i\mathbf{q}\mathbf{r}) \varphi_{xnlm}(\mathbf{r})) d^3\mathbf{r} \right|^2 = \\ &= \frac{2}{\pi} \sum_{m=-l}^{m=l} \left| \sum_{l_k=0}^{l_k=L_{\max}} \sum_{k=0}^{k=l} (2l_q+1) \sqrt{\frac{1}{(2l_k+1)}} \times \right. \end{aligned}$$

⁹ The following remark can be made concerning the numerical results of this work. The calculations of basic components that determine the cross-section of inelastic electron scattering by the atomic nucleus (the function of the perturbed distribution $G_{xnl}(k, k', K)$ and the function $P(k, k')$) are rather simple to be checked: the calculations of those functions can be subjected to a direct and independent mathematical verification [31]. While calculating the cross-section of high-energy electron scattering by nuclei, the most unexpected turned out the fact that a possible error of calculations was highly probable to be hidden in rather simple calculations of simple multipliers entering formula (2) for the cross-section of nuclear electro-disintegration (for instance, this is function $S_x(k, k', K)$ defined in Eq. (6)). The verification of the discussed calculations with the help of a calculator is, as a rule, inefficient: the author reproduced (not without the calculator help) the same errors that were made, when programming the problem. Considering the importance of specific calculations for the comparison of the obtained theoretical results with experimental data, the reproduction of calculation results obtained by different scientific groups, which used independently created software programs, should be regarded as the most reliable means in this case.

Table 9. Specific excitation cross-sections $\sigma_{nl(n) \rightarrow NL(n)}^{ur}$ of proton Coulomb resonances at the inelastic electron scattering by the ^{119}Sn nucleus at the angle $\theta' = 10^{-12}$ deg $\lll \frac{m\omega}{\epsilon\epsilon'}$. The depth parameter of the Woods–Saxon potential $V_{0p} = 58.6$ MeV. The energy of bombarding electrons $\epsilon = 500$ MeV

$[pnl] \downarrow$	$[pNL \rightarrow] 15$	23	13	16	17
10	2.721×10^{-6}	8.558×10^{-4}	3.7342×10^{-5}	5.4054×10^{-7}	6.4525×10^{-6}
11	1.186×10^{-4}	7.352×10^{-3}	6.6438×10^{-3}	1.2378×10^{-5}	1.2662×10^{-4}
12	5.630×10^{-3}	2.505×10^{-2}	2.9398×10^{-3}	2.8603×10^{-4}	4.0838×10^{-4}
20	1.865×10^{-7}	6.661×10^{-3}	2.5291×10^{-2}	1.1900×10^{-5}	5.7686×10^{-4}
13	0.298	0.203	1.3172×10^{-2}	9.9552×10^{-3}	1.1255×10^{-3}
21	1.703×10^{-6}	0.241	0.2899	8.6609×10^{-5}	1.0697×10^{-3}
14	29.83	2.5605	3.6267×10^{-3}	0.4062	1.9780×10^{-2}

$$\begin{aligned} & \times (i)^{l_q+l_k} (-1)^{l_k} \langle (l_k - l + 2k) 0 \ 0 | l_k 0 \rangle \times \\ & \times \langle (l_k - l + 2k) 0 \ l m | l_k m \rangle \times \\ & \times B_{l_k l_q}(K, q, nl) Y_m^{l_k*}(\nu_{\mathbf{k}})^2. \end{aligned} \quad (41)$$

The experiment [10] shows that the cross-section of inelastic high-energy electron scattering by nuclei substantially grows for all atomic nuclei without exceptions if the angle of the inelastic electron scattering decreases. The theoretical calculations [8, 9] interpret the experiment [10] invariantly, if the scattering angle of electrons diminishes substantially. Since there exists a certain probability of and even an urgent necessity in the extension of experimental researches dealing with the inelastic scattering of electrons to the region of small and extremely small scattering angles, the authors developed the method of calculation for such angles ($\theta' \lesssim 10^{-10}$ deg), and the corresponding preliminary calculations were carried out [31].

While comparing the obtained results, first of all, we focus attention on a nontrivial difference between the measurement units (nanobarn/steradian at $\theta' = 60^\circ$ and barns at $\theta' = 10^{-12}$ deg)¹⁰ used to measure identical quantities (the excitation cross-sections of Coulomb resonances) in two above-specified variants of electron scattering. By the way, it is the function $P(\mathbf{k}, \mathbf{k}')$ determined in Eq. (7) that

¹⁰ The difference between measurement units for specific cross-sections is insignificant in this case, because the specific cross-sections that are measured in the nb/sr units can be easily transformed into the simple nb units for the known experimental geometry (we suppose that $\Delta\Omega_{\text{exper}} \lll 1$).

is almost completely responsible for the indicated difference.

Another unordinary and undoubtedly established difference (see Table 9) consists in the evident domination of the excitation (owing to dipole transitions) cross-sections of Coulomb resonances over the cross-sections associated with transitions of higher multipolarities when electrons are inelastically scattered at extremely small angles ($\theta' \lll 1$). In other words, the transition multipolarity plays a leading role in this case ($\theta' \lll 1$). Note also that, in this case, all the responsibility for the phenomenon concerned belongs to another function, namely, $G_{xnl}(\mathbf{q}, \mathbf{K})$, defined in equality (8). It is also worth noting that the result mentioned above does not depend on the error in the coefficient in front of the product of functions $P(\mathbf{k}, \mathbf{k}')$ and $G_{xnl}(\mathbf{q}, \mathbf{K})$.

Note that it is the unordinary magnitudes of excitation cross-sections of Coulomb resonances (tens and hundreds of barns for the analyzed scattering kinematics) that determine the nontrivial capabilities for those resonances to considerably affect the flow of the electro-disintegration processes of atomic nuclei at the inelastic high-energy electron scattering. Note also that the determination of the potential parameters in the extended shell and other models of atomic nuclei substantially depends not least on the capabilities of corresponding nuclear experiments.

Using empirical formulas for the mean free path of an electron in the atomic nucleus, we may assert that a relativistic electron, when moving, e.g., in the atomic nucleus ^{119}Sn , penetrates through its center rather freely. From Table 9, it follows that the cross-sections of electro-disintegration of internal shells in ^{119}Sn , i.e. the knockout of protons from

the deep shells of this nucleus, are too small to considerably change the trajectory at the recurrent inelastic electron scattering by a proton in an internal shell of ^{119}Sn . The result of the collision between a relativistic electron and one of 10 protons of the $p1f$ -shell (in our model, $xnl = p14$) can be the only exception to this statement in the framework of the applied shell model. The theory predicts that the probability of such a collision is extremely high, because the excitation cross-section of the Coulomb $p1G$ -resonance has an improbably huge (as in the case of electromagnetic interaction) value: tens and even hundreds of barns. There is no doubt that this non-trivial result has to manifest itself in various aspects of the theory of inelastic high-energy electron scattering by nuclei.

The result obtained above also serves a basis for the evident interpretation of the giant dipole resonance phenomenon just in the framework of the nuclear shell model. At least, no doubt arises concerning the qualitatively (and even quantitatively) correct interpretation of a decrease in the giant dipole resonance energy as the atomic weight of a chemical element grows. Note, for example, that the excitation energy $\omega_{[r]}$ of Coulomb resonances in the nuclear shell model decreases from about 20 MeV in the ^{12}C nucleus to about 7 MeV in the ^{208}Pb one. Note once again that the physical (quantum-mechanical) properties of quasireal ($q_\mu^2 \approx 0$) and real ($q_\mu^2 \equiv 0$) photons are almost identical in the atomic nuclear region.

Hence, the theory of inelastic high-energy electron scattering by nuclei points to another alternative approach in the interpretation of the giant dipole resonance phenomenon and correctly reproduces the well-known experimental data associated with this electro-nuclear phenomenon at the qualitative level. Note also that, as follows from this statement, in order to experimentally study the giant dipole resonance phenomenon in the framework of the nuclear shell model, the processes of inelastic high-energy electron scattering at small and extremely small angles can be used as well.

1. A.G. Sitenko and V.N. Gur'yev, Zh. Eksp. Teor. Fiz. **39**, 1208 (1960).
2. K.W. McVoy and L. Van Hove, Phys. Rev. **125**, 1034 (1962).
3. R.S. Willey, Nucl. Phys. **40**, 529, (1963).
4. W. Czyż, Phys. Rev. **131**, 2141 (1963).
5. V. Devanathan, Ann. Phys. **43**, 74 (1967).
6. V.K. Tartakovskii and A.A. Pasichnyi, Ukr. Fiz. Zh. **13**, 1361 (1968).
7. A.A. Pasichnyi and V.K. Tartakovskii, Ukr. Fiz. Zh. **13**, 2013 (1968).
8. A.G. Sitenko, A.A. Pasichnyi, and V.K. Tartakovskii, Yadern. Fiz. **12**, 1208 (1970).
9. A.A. Pasichnyi, Ukr. Fiz. Zh. **17**, 1130 (1972).
10. N.G. Afanas'ev, I.M. Arkatov, V.G. Vlasenko, V.A. Gol'dshteyn, S.V. Dementii, E.L. Kuplennikov, V.I. Ogurtsov, and V.I. Startsev, *Preprint KhFTI74-7* (Khar'kov Fiz. Tekhn. Univ., Khar'kov, 1974) (in Russian).
11. R.R. Whitney *et al.*, Phys. Rev. C **9**, 2230 (1974).
12. L.F. Mattheiss, J.H. Wood, and A.C. Switendick, in *Methods in Computational Physics, Vol. 8*, edited by B. Alder, S. Fernbach, and M. Rotenberg (Academic Press, New York, 1968), p. 63.
13. J. Moygey *et al.*, Nucl. Phys. A **262**, 461 (1976).
14. A.A. Pasichnyi, Ukr. Fiz. Zh. **22**, 2039 (1977).
15. V.V. Balashov, *Quantum Theory of Collisions* (Moscow Univ., Moscow, 1985) (in Russian).
16. J.S. O'Connell *et al.*, Phys. Rev. C **35**, 1063 (1987).
17. A.G. Sitenko, A.I. Akhiezer, and V.K. Tartakovskii, *Nuclear Electrodynamics* (Springer, Berlin, 1994).
18. A.A. Pasichnyi, Yadern. Fiz. **54**, 1543 (1991).
19. A.A. Pasichnyi, Ukr. Fiz. Zh. **37**, 487 (1992).
20. M. Zhongyu and F. Dachun, Phys. Rev. C **45**, 811 (1992).
21. G. Garino *et al.*, Phys. Rev. C **45**, 780 (1992).
22. V.R. Pandharipande and S.C. Pieper, Phys. Rev. C **45**, 791 (1992).
23. A.A. Pasichnyi, Ukr. Fiz. Zh. **38**, 1619 (1993).
24. D.B. Day *et al.*, Phys. Rev. C **48**, 1849 (1993).
25. C.F. Williamson *et al.*, Phys. Rev. C **56**, 3152 (1997).
26. D. Dutta *et al.*, Phys. Rev. C **61**, 061602 (2000).
27. A. Meucci, C. Giusti, and F.D. Pacati, Phys. Rev. C **64**, 014604 (2001).
28. O. Benhar, D. Day, and I. Sick, Rev. Mod. Phys. **80**, 189 (2008).
29. A.A. Pasichnyi and O.A. Prygodiuk, Yadern. Fiz. **68**, 2051 (2005).
30. A.A. Pasichnyi, Elem. Chast. At. Yadr. **41**, 197 (2010).
31. A.A. Pasichnyi and O.A. Prygodiuk, Open J. Microphys. **3**, 12 (2013).
32. K.N. Mukhin, *Experimental Nuclear Physics, Vol. 1. Physics of Atomic Nucleus* (Moscow, Mir, 1987).
33. J.J. Sakurai, *Advanced Quantum Mechanics* (Addison-Wesley, Reading, Massachusetts, 1967).
34. V.B. Berestetskii, E.M. Lifshitz, and L.P. Pitaevskii, *Relativistic Quantum Theory* (Pergamon Press, Oxford, 1982).

35. A.I. Baz, Ya.B. Zeldovich, and A.M. Perelomov, *Scattering, Reactions and Decays in Non-Relativistic Quantum Mechanics* (Israel Program for Sci. Transl., Jerusalem, 1969).
36. D.A. Varshalovich, A.N. Moskalev, and V.K. Khersonskii, *Quantum Theory of Angular Momentum* (World Scientific, Singapore, 1988).
37. S.E. Koonin, *Computational Physics* (Addison-Wesley, Reading, MA, 1986).
38. H.F. Lutz and M.D. Karvelis, *Nucl. Phys.* **43**, 31 (1963).

Received 18.11.12.

Translated from Ukrainian by O.I. Voitenko

А. Пасічний, О. Пригодюк

КУЛОНІВСЬКІ РЕЗОНАНСИ,
КВАЗІРЕАЛЬНІ ФОТОНІ І ФЕНОМЕН
ДИПОЛЬНОГО ГІГАНТСЬКОГО РЕЗОНАНСУ

Р е з ю м е

В рамках оболонкової моделі ядер вивчені різноманітні аспекти впливу квазіреальних фотонів та кулонівських резонансів на динаміку електродезінтеграції ядер при непружному розсіянні електронів високих енергій. Деякі особливості чисельних методів, що використовуються для вивчення перерізів електророзщеплення атомних ядер електронами високих енергій, також представлені в даній роботі.